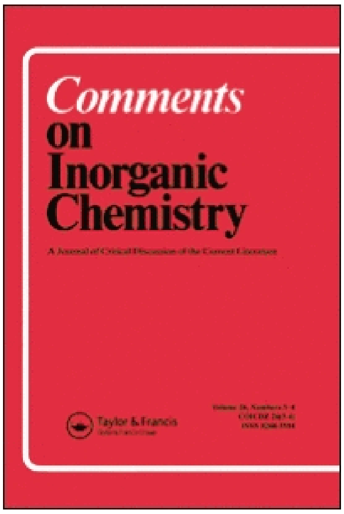

Comments on Inorganic Chemistry

Publication details, including instructions for authors and subscription information:
http://www.informaworld.com/smpp/title~content=t713455155

Electronic Absorption-Charge Transfer Transitions

To cite this Article (1984) 'Electronic Absorption-Charge Transfer Transitions', Comments on Inorganic Chemistry, 3: 5, 249 — 260

To link to this Article: DOI: 10.1080/02603598408080075

URL: http://dx.doi.org/10.1080/02603598408080075

10. E. I. Solomon, J. W. Hare, D. M. Dooley, J. H. Dawson, P. J. Stephens, and H. B. Gray, J. Am. Chem. Soc. **102**, 168 (1980), and references therein.
11. (a) D. W. Smith, Inorg. Chim. Acta **22**, 107 (1977).
(b) M. Gerloch, J. H. Harding, and R. G. Wooley, Struct. Bond. **46**, 1 (1981).
12. S. R. Desjardins, K. W. Penfield, S. L. Cohen, R. L. Musselman, and E. I. Solomon, J. Am. Chem. Soc. **105**, 4590 (1983).

IV. ELECTRONIC ABSORPTION—CHARGE TRANSFER TRANSITIONS

A. Basic Principles

When the absorption spectrum of $CuCl_4^=$ is extended to energies higher than those associated with the $d \rightarrow d$ transitions, new, extremely intense absorption bands are observed. These are Laporté-allowed charge-transfer transitions which result from optical excitation of an electron from the valence $3p$ orbitals on the chloride ligands into the half-occupied $d_{x^2-y^2}$ orbital on the copper ion. Interpretation of the energy and intensity of these ligand-to-metal charge transfer transitions requires that the energy level diagram in Figure III-1 now be extended to include the valence orbitals on the four chloride ligands.

In D_{4h}-$CuCl_4^=$, each chloride ligand donates three $3p$ valence orbitals, one of which participates in a σ type of bonding interaction along the Cl–Cu bond, the other two being perpendicular to the Cl–Cu bond and involved in in-plane-(h) and out-of-plane-(v) π type bonding with the copper (Figure IV-1). Treating the equivalent orbitals on the four Cl^- ligands together, nine different symmetry-adapted linear combinations of ligands orbitals, χ_L, are obtained.[2] These are given in Figure IV-1. In the $CuCl_4^=$ complex these ligand-orbital combinations are split in energy both due to ligand-ligand interactions and bonding interactions of χ_L with metal-centered orbitals of the same symmetry. Consideration of these interactions results in the qualitative molecular-orbital energy level ordering shown in Figure IV-2. The specific order and quantitative splitting of the levels can be very dependent on the type of molecular bonding calculation used. Thus it is critical that the calculated energy level diagram be evaluated experimentally. Excitation of electrons from the filled ligand-centered orbitals into the hole in the copper $d_{x^2-y^2}$ produces the charge-transfer excited states indicated to the right of

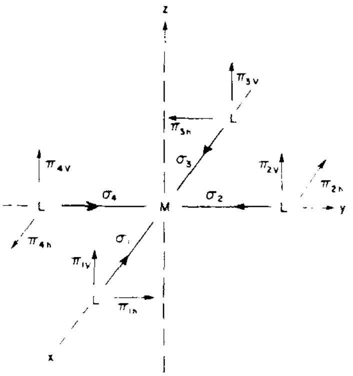

χ_L

pΠ (in-plane)	$a_{2g} \rightarrow$	$\frac{1}{2}(\Pi_{1h} + \Pi_{2h} + \Pi_{3h} + \Pi_{4h})$
	$b_{2g} \rightarrow$	$\frac{1}{2}(\Pi_{1h} - \Pi_{2h} + \Pi_{3h} - \Pi_{4h})$
	$e_u \rightarrow$	$\frac{1}{\sqrt{2}}(\Pi_{1h} - \Pi_{3h})$ $\frac{1}{\sqrt{2}}(\Pi_{2h} - \Pi_{4h})$
pΠ (out-of-plane)	$a_{2u} \rightarrow$	$\frac{1}{2}(\Pi_{1v} + \Pi_{2v} + \Pi_{3v} + \Pi_{4v})$
	$b_{2u} \rightarrow$	$\frac{1}{2}(\Pi_{1v} - \Pi_{2v} + \Pi_{3v} - \Pi_{4v})$
	$e_g \rightarrow$	$\frac{1}{\sqrt{2}}(\Pi_{1v} - \Pi_{3v})$ $\frac{1}{\sqrt{2}}(\Pi_{2v} - \Pi_{4v})$
pσ	$a_{1g} \rightarrow$	$\frac{1}{2}(\sigma_1 + \sigma_2 + \sigma_3 + \sigma_4)$
	$b_{1g} \rightarrow$	$\frac{1}{2}(\sigma_1 - \sigma_2 + \sigma_3 - \sigma_4)$
	$e_u \rightarrow$	$\frac{1}{\sqrt{2}}(\sigma_1 - \sigma_3)$ $\frac{1}{\sqrt{2}}(\sigma_2 - \sigma_4)$

FIGURE IV-1 Symmetry-adapted linear combinations of ligand valence orbitals for D_{4h}–$CuCl_4^{=}$ (taken from Ref. 1).

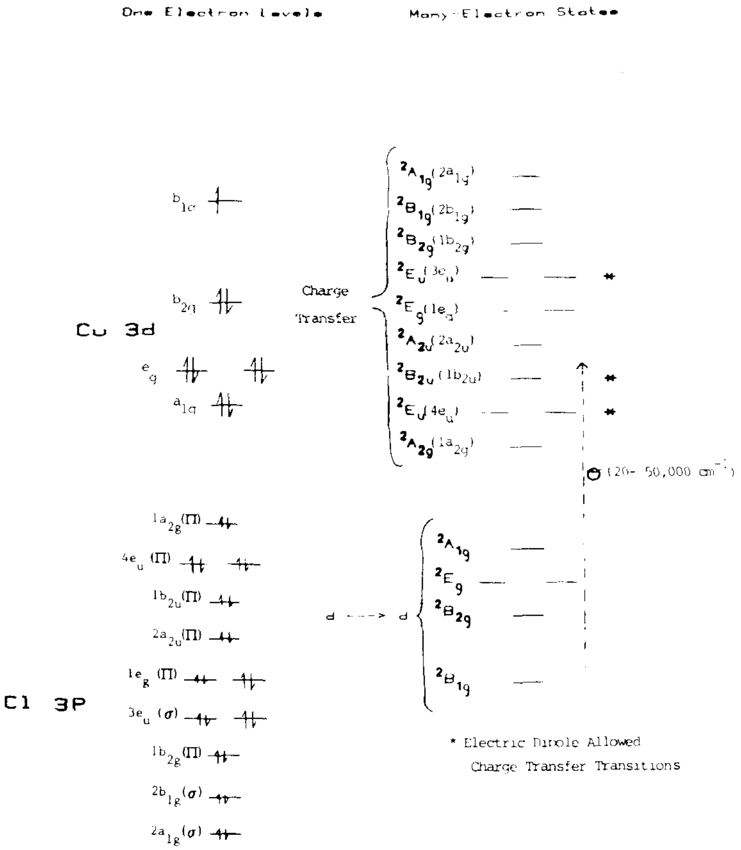

FIGURE IV-2 Charge-transfer excited states of D_{4h}–$CuCl_4^=$: Extension of Figure III-1 to include transitions from the $3p$ valence orbitals of the four chloride ligands.

Figure IV-2. These can be probed in detail by electronic absorption spectroscopy.

The intensity with which the nine charge-transfer transitions can contribute to the absorption spectrum is again dependent on the electric dipole transition moment integral, $\int \psi_g M(x,y,z)\psi_e d\tau$ in Eq. (III-1b). For D_{4h}–$CuCl_4^=$, group theory indicates that three transitions are electric dipole allowed: two $^2B_{1g} \rightarrow {}^2E_u$ transitions which are x,y polarized, and the $^2B_{1g} \rightarrow {}^2B_{2u}$ transition which is allowed when the $\vec{E}$ vector of light is oriented along the molecular z axis. The remaining charge-transfer transitions are forbidden but can still contribute to the absorption spectrum, with several orders of magnitude lower intensity, through vibronic coupling or through static distortion of the $CuCl_4^=$ complex to a symmetry lower than D_{4h}.

The above selection rules derive only from group theory. It is also important to quantitatively consider the charge-transfer transition *intensity*, as this directly relates to the overlap between ligand χ_L and metal ϕ_M orbitals. Upon bonding, the wavefunctions associated with the molecular orbitals of the complex become $\Phi = C_M \phi_M + C_L \chi_L$ where the C's are the normalized coefficients of mixing. The electric dipole transition moment occurring in Eq. (III-1b) can now be written as an integral over the one-electron molecular orbitals involved in the transition of the electron from the ground to excited state.

$$\int \Phi_g \vec{r} \, \Phi_e d\tau = C_M^g C_M^e \int \phi_M^g \vec{r} \, \phi_M^e \, d\tau + C_M^g C_L^e \int \phi_M^g \vec{r} \, \chi_L^e d\tau + C_L^g C_M^e \int \chi_L^g \vec{r} \, \phi_M^e d\tau + C_L^g C_L^e \int \chi_L^g \vec{r} \, \chi_L^e d\tau. \tag{IV-1}$$

Here Φ_g is a one-electron molecular orbital dominantly on the ligand and Φ_e is the b_{1g} molecular orbital dominantly on the copper. The first term in the expansion must be zero for metal-centered d orbitals. Generally, calculations[3] indicate that it is the last term which dominates the intensity of charge-transfer transitions. This involves only contributions from chloride-centered χ_L in the one-electron molecular orbitals of the ground and excited states. Hence, in order to have transition intensity, C_L^e must be greater than zero and thus there must be some mixing of the χ_L^e having b_{1g} symmetry into the copper $d_{x^2-y^2}$ orbital. Note that this mixing is also required by the g values obtained from EPR spectroscopy in Section II-C. Further, if contributions due to overlap of p orbitals on adjacent ligands are neglected, the following relation is obtained[3,4]:

$$\int \chi_L^g \vec{r} \, \chi_L^e d\tau \cong \sum_{\alpha=1}^{4} k_\alpha^g k_\alpha^e \, \vec{r}_\alpha \, \delta_{g,e} \tag{IV-2}$$

In Eq. (IV-2), α are the four ligands, k_α is the coefficient of ligand α in the χ_L, $\vec{r}_\alpha$ is the position vector of ligand α taken from the metal center, and $\delta_{g,e}$ derives from overlap of orbitals on a given ligand in the molecular orbitals associated with the ground and excited states. Within this approximation, transition intensity requires that the same type of orbital ($p\sigma$, $p\pi_h$, or $p\pi_v$) must be present on a given ligand in both the ground and excited states.

In summary, the charge-transfer transition energies and intensities are sensitive probes of metal-ligand bonding interactions in complexes which enable an accurate evaluation of the results of molecular orbital calculations.

B. The Experiment

Polarized single-crystal electronic absorption spectral studies in the charge-transfer region parallel those outlined for $d \rightarrow d$ transitions in Section III-B with additional complications associated with the very high ϵ values of some of these Laporté-allowed transitions. It is unrealistic to polish a crystal to less than 2μ thickness without generating cracks which cause stray light problems that distort the absorption band. This places limits on the ϵ values accessible by absorption spectroscopy on pure single crystals of metal complexes. (For a 2μ thick crystal, with a concentration of complex $= 3.7$ g cm^{-3}, an absorbance of 2 corresponds to an $\epsilon = 300$.) Two approaches are generally taken to overcome this problem. The first is to grow doped crystals of a spectroscopically transparent isomorphous host which have small percentages of the complex of interest homogeneously dispersed, and therefore at lower concentration. This requires that the structure of the complex in the host lattice be the same as in the pure material. Alternatively, polarized spectral studies can be performed directly on single crystals of the pure material using the technique of specular reflectance spectroscopy.[5] Here, light is again propagated incident to the crystal face, but now the reflected light is detected. The absorption spectrum is then obtained through a Kramers-Kronig transformation of the reflection data. This transformation requires an integration of the reflectivity over all energies. Since intense allowed transitions must exist in the vacuum UV which are not readily accessible experimentally (see Section V), these must be approximated in this integration by an effective reflectivity peak at high energy. This, however, can be reasonably fit so as to give a zero value of ϵ in the Kramers-Kronig transformed absorption spectrum in the low energy nonabsorbing region. The sensitivity of reflectivity measurements increases as the ϵ of an absorption band increases. With a lower limit of $\epsilon = 200$, this method provides an important complement to direct polarized single-crystal absorption studies. One complication associated with studies of pure materials must be realized. As ϵ's become quite high ($> 2{,}000$), intermolecular coupling of transitions can occur which produces exciton effects[6] that can distort the molecular absorption spectrum.

The polarized single crystal absorption spectrum of the charge-transfer region of D_{4h}–$CuCl_4^=$ is shown[7] in Figure IV-3. Two dominant absorption bands are observed, one at ~26,500 cm^{-1} and a second at ~36,000 cm^{-1}. These are xy polarized and split by the lower-than-D_{4h} site symmetry of the $CuCl_4^=$ complex in the crystal. Thus they must be assigned as the $^2B_{1g} \rightarrow {}^2E_u$ transitions. No significant intensity is observed in z polarization. At higher sensitivity in Figure IV-3b, the lowest energy charge-transfer transition at ~23,000 cm^{-1} is observed. It is xy polarized but unsplit by the low $CuCl_4^=$ site symmetry and thus is a nondegenerate, forbidden charge-transfer transition made allowed by vibronic coupling. Detailed studies of the energy of this band in different D_{4h}–$CuCl_4^=$ crystal lattices indicate it to be the $^2B_{1g} \rightarrow {}^2A_{2g}$ transition.

C. Comparison of Experiment and Theory

As indicated in Section IV-A, detailed spectroscopic studies of the charge-transfer transitions allow an accurate evaluation of the results of molecular bonding calculations. The results of an SCF-Xα-SW transition state calculation[7] of the charge-transfer transitions of D_{4h}–$CuCl_4^=$ are given in Table IV-1. The experimental energies given in the third column come from the polarized single crystal spectrum assigned in Figure IV-3. For the three charge-transfer transitions observed, the calculated energies are significantly lower than those obtained from experiment. Alternatively, the last two columns indicate that there is good quantitative agreement between the observed and calculated charge-transfer energy differences. As these differences reflect the splittings of the ligand orbitals, this agreement supports the results of the calculation in evaluating ligand-ligand interactions and bonding interactions with the metal ion. A rough estimate of the relative magnitude of these interactions can be obtained from a

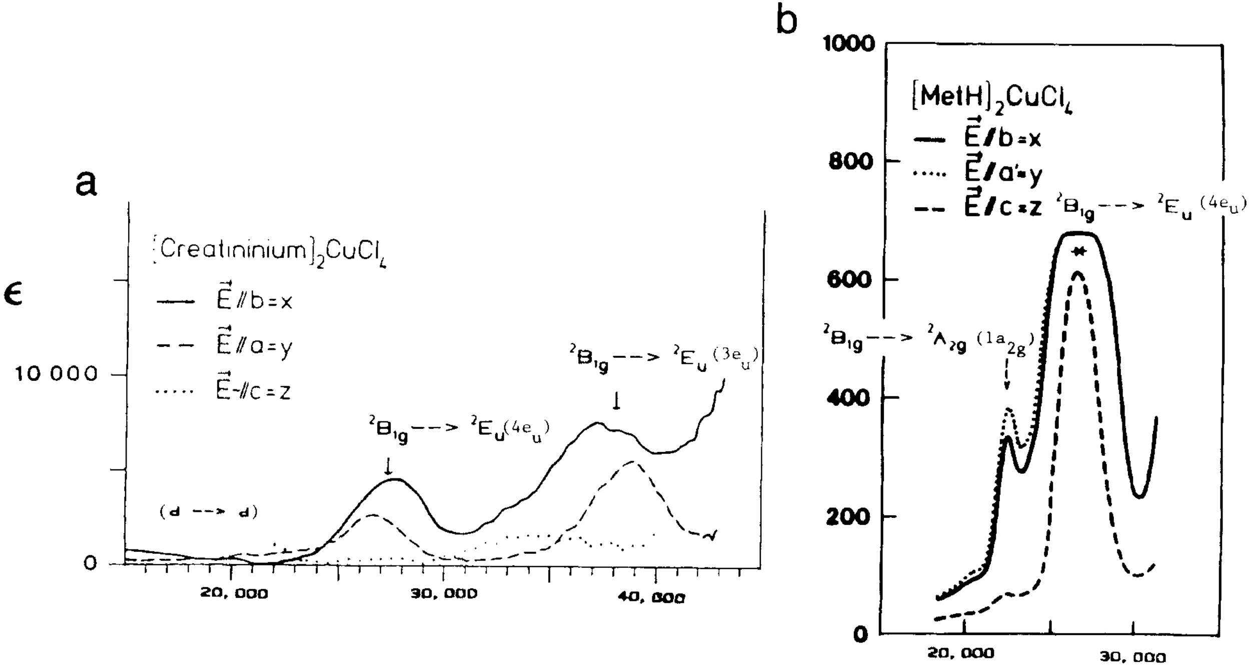

FIGURE IV-3 Polarized single crystal spectra of charge transfer region of D_{4h}–$CuCl_4^{=}$: (a) Kramers-Kronig transformation of specular reflectance data. (b) At higher sensitivity, absorption spectrum of low energy part of the charge transfer region. *a*, *b*, and *c* refer to crystal axes and *x*, *y*, and *z* refer to molecular axes.

* Note top of absorption band distorted by stray light problem.

TABLE IV-1

SCF-Xα-SW transition state calculations of the charge-transfer spectra of D_{4h}–$CuCl_4^{=}$

D_{4h} $CuCl_4^{=}$ All possible CT Transitions	SCF-Xα-SW calculated transition energy (cm^{-1})	Experimentally observed transition energy (cm^{-1})	Transition energy differences	
			Calculated	Observed
${}^2A_{2g} \leftarrow {}^2B_{1g}\ (1a_{2g} \rightarrow 3b_{1g})\pi$	16,870	23,700	0	0
${}^2E_u \leftarrow (4e_u \rightarrow\ )\pi + \sigma$	20,430	26,400	3,650	2,700
${}^2B_{2u} \leftarrow (1b_{2u} \rightarrow\ )\pi$	21,550	[a]		
${}^2A_{2u} \leftarrow (2a_{2u} \rightarrow\ )\pi$	26,960			
${}^2E_g \leftarrow (1e_g \rightarrow\ )\pi$	28,130			
${}^2E_u \leftarrow (3e_u \rightarrow\ )\sigma + \pi$	30,010	35,900	13,140	12,220
${}^2B_{2g} \leftarrow (1b_{2g} \rightarrow\ )\pi$	31,450			
${}^2B_{1g} \leftarrow (2b_{1g} \rightarrow\ )\sigma$	34,880			
${}^2A_{1g} \leftarrow (2a_{1g} \rightarrow\ )\sigma$	39,570			

[a] Allowed but not observed.

weighted average of the results in Table IV-1: σ-π splitting ~7500 cm^{-1}, L-L splitting ~10-13000 cm^{-1}. Hence both contribute significantly to the energy splittings of the charge-transfer transitions. Figure II-6 can now be extended to include the SCF-Xα-SW generated wavefunctions of the observed charge-transfer excited states (Figure IV-4).

There has been some interest in correlating the changes in energy of charge-transfer transitions with geometry.[8] This can be evaluated both experimentally and theoretically for a distortion of $\mathrm{CuCl_4}^{=}$ from D_{4h} to D_{2d}. The results[7,9] are given in Figure IV-5. One model which has been used assumes that all change in charge-transfer energy derives from the change in energy of the half-occupied $d_{x^2-y^2}$ orbital due to the change in ligand field as discussed in Section III-C. This ligand-field model, which requires that the ligand-derived molecular energy levels in Figure IV-2 do not change energy upon distortion, predicts all D_{4h}–$\mathrm{CuCl_4}^{=}$ transitions to shift to lower energy by ~5000 cm^{-1}. From Figure IV-5, correlation of the three observed charge-transfer transitions in D_{4h}–$\mathrm{CuCl_4}^{=}$ to the analogous transitions in the D_{2d} complex indicates that all do shift to lower energy, but by significantly different amounts ($^2A_2$ by 1000 cm^{-1}, $^2E(\pi)$ by 1700 cm^{-1}, $^2E(\sigma)$ by 2400 cm^{-1}). These differences from the ligand-field prediction dominantly result from changes upon distortion in ligand-ligand repulsion for the wavefunctions shown in Figure IV-4. Thus, the correlation of charge-transfer transition energies with geometry is more complex than the geometric effects on the $d \rightarrow d$ transitions discussed in Section III-C.

The intensities of the group-theoretically-allowed charge-transfer transitions have been calculated as discussed in Section IV-A, using the SCF-Xα-SW wavefunctions in Figure IV-4. These results[7] are compared with experiment in Table IV-2. The reasonable agreement between theory and experiment gives some confidence in the coefficients of mixing of these wavefunctions which were used in Eq. (IV-1). It should be emphasized that these calculations predict no intensity in the $^2B_{1g} \rightarrow {}^2B_{2u}$ transition which is group theoretically allowed in z polarization but not experimentally observed (Figure IV-3).

The b_{1g} orbital in D_{4h} has contributions only from the χ_L derived from the Cl $p\sigma$ orbitals (Figure IV-1). In the model discussed in Section IV-A the intensity is derived from overlap of the ligand $3p$ orbitals in the ground and excited states. Together, these considerations place strong requirements on the nature of the ligand character

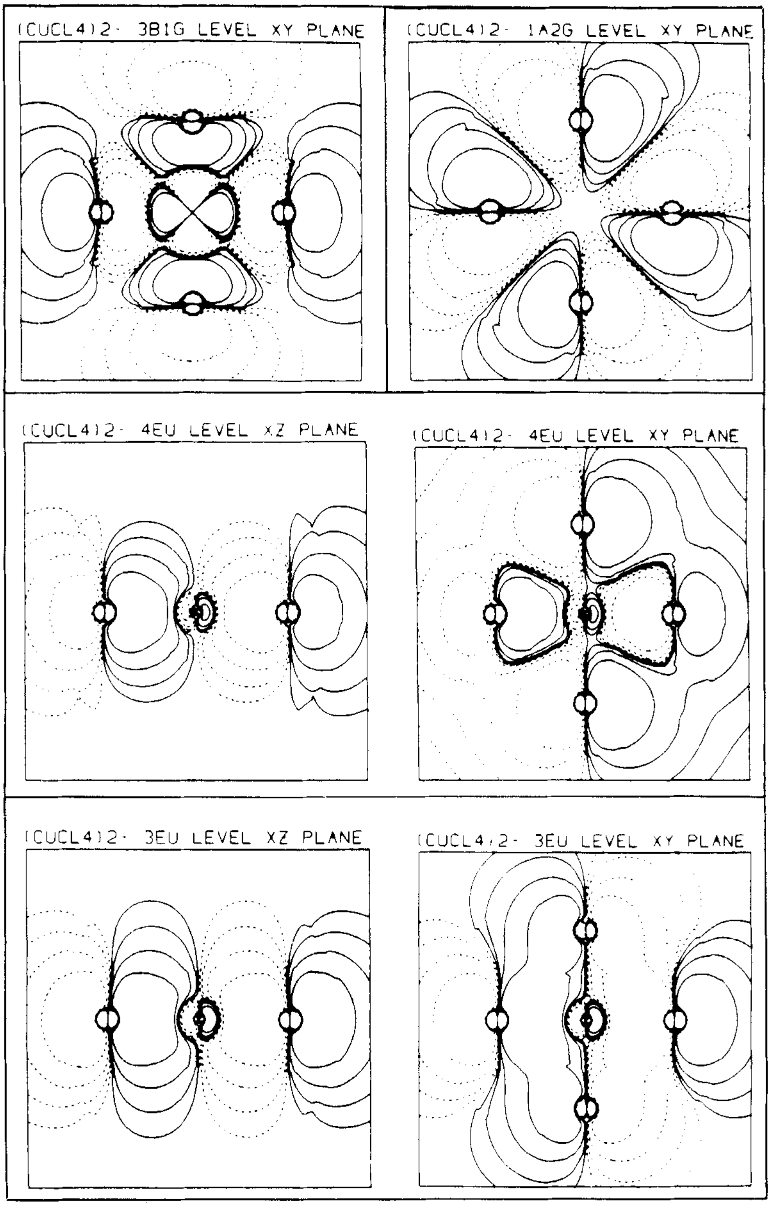

FIGURE IV-4 SCF-Xα-SW contour diagrams of the observed charge–transfer levels of D_{4h}–$CuCl_4^{=}$. Coordinates as in Figure II-6.

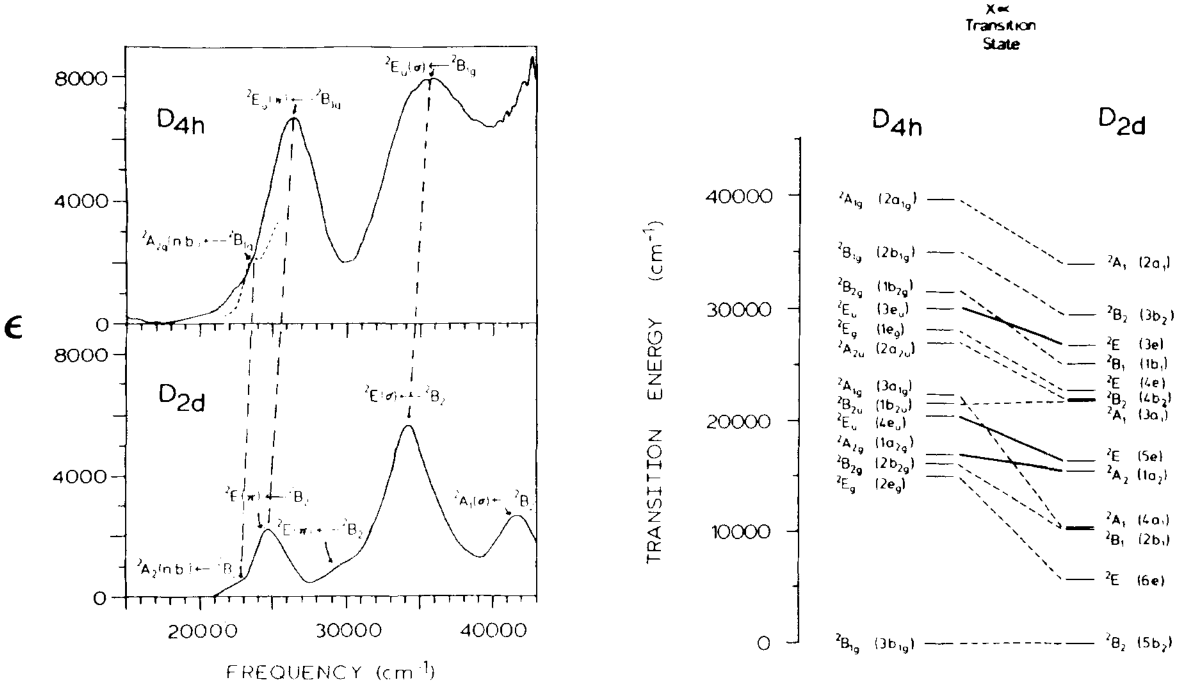

FIGURE IV-5 Effects of a distortion from D_{4h} to D_{2d} on the charge transfer spectrum of $CuCl_4^=$. Experiment (left) and SCF-Xα-SW transition state calculations (right).

TABLE IV-2
SCF-Xα-SW calculated and observed oscillator strengths for symmetry allowed charge-transfer transitions of D_{4h}-$CuCl_4^=$

Transition	Frequency (cm^{-1})[a]	Oscillator strength[b]	
		Theoretical	Experimental
$1b_{2u} \rightarrow 3b_{1g}$	27,520[c]	0.0	0.0
$4e_u \rightarrow 3b_{1g}$	26,400	0.104	0.055
$3e_u \rightarrow 3b_{1g}$	37,400	0.355	0.405

[a] For transitions from e_u orbitals, the frequency of the x-polarized transition is given.
[b] For transitions from e_u orbitals, only the x-polarized component of both the theoretical and experimental oscillator strength is given.
[c] Value estimated from $X\alpha$ transition-state calculations.

in the orbital from which the excited electron originates, in order to have charge-transfer intensity. The $3e_u(\sigma)$ level has 70% $p\sigma$ character making the ${}^2B_{1g} \rightarrow {}^2E_u(\sigma)$ transition quite intense, while the ${}^2B_{1g} \rightarrow {}^2E_u(\pi)$ transition associated with the $4e_u(\pi)$ level acquires intensity by configurational mixing of $p\sigma$ character from ${}^2E_u(\sigma)$. Since the $1b_{2u}$ orbital contains no Cl $p\sigma$ character (Figure IV-1) it has no overlap with the $3b_{1g}$ ligand orbitals and thus the ${}^2B_{1g} \rightarrow {}^2B_{2u}$ transition has no intensity even though it is allowed by group theory.

References

1. C. J. Ballhausen and H. B. Gray, J. Am. Chem. Soc. **85**, 260 (1963).
2. F. A. Cotton, *Chemical Applications of Group Theory*, 2nd ed. (Wiley-Interscience, New York, 1971), Chapter 6.
3. A. Avoird and P. Ros, Theoret. Chim. Acta **4**, 13 (1966).
4. M. Wolfsberg and L. Helmholtz, J. Chem. Phys. **20**, 837 (1952).
5. (a) G. Kortum, *Reflectance Spectroscopy* (Wiley-Interscience, New York, 1966).
   (b) B. G. Anex, Mol. Cryst. **1**, 1 (1966).
6. (a) D. L. Dexter and R. S. Knox, *Excitons* (Wiley-Interscience, New York, 1965).
   (b) A. S. Davydov, *Theory of Molecular Excitons* (McGraw-Hill, New York, 1962).
   (c) D. P. Craig and S. H. Walmsley, *Excitons in Molecular Crystals*, (W. A. Benjamin, New York, 1962).
7. S. R. Desjardins, K. W. Penfield, S. L. Cohen, R. L. Musselman, and E. I. Solomon, J. Am. Chem. Soc., **105**, 4590 (1983).
8. H. J. Schugar, in *Copper Coordination Chemistry: Biochemical & Inorganic Perspectives*, edited by K. D. Karlin and J. Zubieta, (Adenine Press, Guilderland, New York, 1983), and references therein.
9. A number of assignments for the charge transfer spectrum of D_{2d}-$CuCl_4^=$ have appeared. The one indicated in Figure IV-5 is most consistent with a correlation from the D_{4h}-$CuCl_4^=$ spectrum and the results of UPS studies (Section VI). See discussion in Ref. 7.